Hindawi
Advances in Materials Science and Engineering
Volume 2020, Article ID 6525096, 10 pages
https://doi.org/10.1155/2020/6525096

Research Article

Physical Simulation on Molten Steel Flow Characteristics of RH Vacuum Chamber with Arched Snorkels

Zhi-Feng Ren,[1,2,3] **Zhi-Guo Luo**,[1] **Fan-Xia Meng**,[4] **Zong-Shu Zou**,[1] **Yi-Hong Li**,[2,3] **Ai-Chun Zhao**,[2,3] **and Hai-Lian Gui**[2,3]

[1]*School of Metallurgy, Northeastern University, Shenyang 110819, China*
[2]*School of Materials Science and Engineering, Taiyuan University of Science and Technology, Taiyuan 030024, China*
[3]*Engineering Research Center Heavy Machinery Ministry of Education, Taiyuan University of Science and Technology, Taiyuan 030024, China*
[4]*State Key Laboratory of Rolling and Automation, Northeastern University, Shenyang 110819, China*

Correspondence should be addressed to Zhi-Guo Luo; luozg@mail.neu.edu.cn and Fan-Xia Meng; 1610196@stu.neu.edu.cn

Received 11 May 2020; Revised 30 July 2020; Accepted 10 August 2020; Published 30 August 2020

Academic Editor: Jan Koci

Copyright © 2020 Zhi-Feng Ren et al. This is an open access article distributed under the Creative Commons Attribution License, which permits unrestricted use, distribution, and reproduction in any medium, provided the original work is properly cited.

The RH vacuum refining technology is a vitally powerful method of producing clean steel. The inner diameter of traditional circular snorkel is very difficult to be increased owing to the metallurgical refractory thickness around the snorkels and the limitation of the area under the vacuum chamber, limiting the increase in refining efficiency. In order to improve the refining efficiency of the RH reactor, a new designed RH degasser with an optimized arched snorkel is established. This design replaces the traditional two circular snorkels structure with the two arched snorkels and greatly enhances the cross-sectional area of snorkel. In this study, the flow characteristics of this new type RH were studied and analyzed by establishing a 1 : 5.5 physical model of RH with arched snorkels. Results show that the circulation flow rate of RH with arched snorkels can increase by 100% ~ 180% and the mixing time approximately decreases by 35% compared with RH with circular snorkels under actual production conditions. The circulation flow rate of RH with arched snorkels continues to increase obviously when gas flow rate exceeds the saturated value of RH with circular snorkels. The RH with arched snorkels can increase the refining efficiency significantly and has important application prospect.

1. Introduction

As a tool for molten steel secondary refining, the Ruhrstahl–Heraeus (RH) processing has wide applications owing to its multiple metallurgical functions, such vacuum degassing, decarburization, inclusion removal, denitrogenation, and inclusion removal. It is widely used for the production of ultralow carbon steels, bearing steels, pipeline steels, spring steels, silicon steels, etc. The RH vacuum steel degassing process depends on sucking the liquid steel from the ladle to the vacuum chamber equipped with two snorkels (up-leg and down-leg) [1]. When the inert gas is blown to the liquid steel, then the circulation flow of steel between vacuum chamber and ladle is forced. The degassing process mainly occurs in liquid internal [1], at splashed metals in vacuum chamber and bubble surfaces [2, 3], which involves complex chemical reactions and transport phenomena [4]. Thus, to improve the degassing and decarburization rate and promote the inclusion removal rate in the RH systems, it is important to illustrate liquid steel flow characteristics. Nevertheless, the RH system can hardly be observed directly because of its complex physical and pyrometallurgical process, which involves thermodynamics, kinetics, and multiphase flow and mass transfer [4]. The problem was suddenly thrown into sharp focus. In order to reduce costs, many researchers are very concerned about improving the refining efficiency of RH equipment. It is generally considered that the circulation flow rate [5–10] and the mixing time [11–16] are two significant parameters during the RH process. Thus, many researchers have developed physical [10, 11, 17–21] or mathematical models [5, 13, 22–27] to simulate the multiphase flow [13, 22, 26–29], mixing

phenomena [10–16, 28–31], behavior of bubble and inclusion removal [22, 30, 32], and decarburization process [1, 2, 8, 20, 23, 25, 33, 34] during the RH treatment. Based on the physical simulation experiment work of predecessors on circulation flow rate of RH, some empirical formulas are listed in Table 1, which includes the formulas put forward at the first time and excludes similar equations reported later. It is generally accepted that the circulation flow rate of RH is related to the injected gas flow rate and the section size of snorkel. From process parameter improvement view, many researches have proved that a higher gas flow rate [5, 7, 29, 30, 34], a lower vacuum pressure [18, 19, 28], a deeper insertion depth of snorkel [3, 14] would favor to optimize the fluid flow of RH. However, the circulation rate will reach a saturated value with the gas flow rate increasing [14, 36]. From equipment improvement view, many investigations have proved that a larger snorkel sectional area [24, 26, 29, 38]blowing from the bottom of the vacuum chamber [15] or ladle [39] would favor to optimize the fluid flow of RH. Recently, many researchers have tried to increase the refining efficiency by using single-leg [12, 28, 31, 40], multilegs [38, 41], and magnetic field [42] imposed around the up-leg. However, the single-leg was hardly used in the actual industrial manufacture considering technical immaturity; meanwhile, multilegs and imposing magnetic field around snorkel were also hardly used in the actual industrial manufacture considering the cost issue. All of the equations in Table 1 imply that the arched snorkels with greater sectional area would bring a larger circulation flow rate. Additionally, the stimulus-response was the general method used to measure the mixing time [7, 10], another important parameter for the RH treatment. In the physical simulation experiments of this paper, this method will continue to observe the mixing of molten steel.

However, little results [38, 42] were reported to study the shape of RH snorkels, which has always been circular until the oval snorkel was proposed by Kuwabara [15]. The oval snorkels were favored to enhance fluid flow of RH, but we want the refining efficiency to keep getting bigger, including a great increase in circulation flow rate and saturated value of gas flow rate. In the current study, a new vacuum degasser equipped with two snorkels of larger sectional area was designed. The two traditional circular snorkels were replaced with two arched snorkels, which was not reported in previous investigations. For the arched snorkel, the internal arc height is equal to the radius of traditional circular snorkel and the internal diameter is 3 to 4 times of the circular snorkel. Hence, the sectional area of arched snorkel is much larger than that of circular snorkel. Water modeling was performed according to similarity criterion. The flow velocity of the RH water model down-on leg-outlet plane was captured by electronic tachometer, and the stimulus-response method was used to measure the mixing time. The results provided the experimental basis for promoting and improving this new RH vacuum refining equipment.

2. Experiment

2.1. Model Design. The prototype is one RH vacuum chamber with two circular snorkels from a steel plant in China. According to the empirical formulas listed in Table 1, we have determined the kernel idea of this design is to increase the cross-sectional area of snorkel as much as possible. The scale of water model and prototype is 1 : 5.5. Figure 1(a) shows the model size of circular snorkel. The circular snorkel diameter is very difficult to be increased owing to the metallurgical refractory thickness around the snorkels and the limitation of the area under the vacuum chamber. In order to increase the cross-sectional area of the snorkel as much as possible, two snorkels are changed to arched structures in this research. So as to make full use of the space under the vacuum chamber, the inner diameter of the vacuum chamber is determined as the diameter of arched snorkel and the arc height is same as the inner diameter of circular snorkel, utilizing the bottom space of the vacuum chamber optimized. Figure 1(b) exhibits the top view of the arched snorkel water model. Compared with circular snorkel, this arched structure increases the equivalent inner diameter by approximately 70% and the cross-sectional area by 193% in this design.

2.2. Similarity Theory. A 1 : 5.5 scale water model of 170 t RH was built according to the similarity principle. Table 2 shows the main parameters of the prototype and physical model. The lifting gas flow rate of model Q_m is calculated from the actual gas flow rate on-site Q_p with the modified Froude criterion according to the following equation:

$$Q_m = 0.01448 Q_p. \tag{1}$$

2.3. Experimental Device and Parameters. The water model experimental devices consist of vacuum chamber and ladle made of plexiglass. Two snorkels are equipped at the bottom of the vacuum chamber. To the RH with two circular snorkels, compressed air is used as the lifting gas through six evenly distributed gas injection nozzles in one horizontal plane of circular up-leg. To the RH with two arched snorkels, four nozzles are distributed evenly in the arc of the arched up-leg, two others are distributed evenly in the chord, and these six nozzles are in one horizontal plane of arched up-leg. This model also includes the gas source system, gas distributor and transmission pipeline, vacuuming system, metering system, and detection system. Figure 2 shows the schematic of the main apparatus of the water model.

The gas flow rate is 60 ~ 130 $Nm^3 \cdot h^{-1}$, the pressure in the vacuum chamber is 67 Pa, and insertion depth of snorkel is 627 mm in the production site. Table 3 shows the corresponding parameters of the prototype and water model.

2.4. Experimental Index

2.4.1. Circulation Flow Rate. The circulation flow rate G_m was obtained by measuring the fluid velocity, which was 20 mm above the outlet of the down-leg. Five measuring points were horizontally and longitudinally set at the cross-sectional center of down-leg. The fluid velocity at the measuring point was obtained with an electronic tachometer

Table 1: Equations for circulation flow rate.

Author	Equations	Variables	Reference
Watanabe et al.	$Q = 0.020D^{1.5}G^{0.33}$	Q: circulation flow rate, t·min^{-1}; G: gas flow rate, NL·min^{-1}; D: diameter of snorkel, m	[35]
Tokio et al.	$Q = K \cdot D^{1.5}G^{0.33}$	K: constant	[11]
Seshadri and Costa	$Q = \rho \cdot S \cdot (0.74G \ln(P_2/P_1))^{1/3}$	ρ: liquid density, g·cm^{-3}; S: section area of snorkel, m^2 P_1: pressure at top level, Pa; P_2: pressure at injection point, Pa	[36]
Kuwabara et al.	$Q = K \cdot G^{1/3}D^{4/3}[\ln P_1/P_2]^{4/3}$	P_1: pressure at blowing point, atm P_2: pressure at vacuum vessel, atm	[15]
Kamata et al.	$Q = 11.4Q_g^{(1/3)}d_p^{(4/3)}(\ln 1 + \rho_1 gh/P_v)^{(1/3)}$	Q_g: gas flow rate, NL·min^{-1}; d_p: diameter of snorkel, m; ρ_l: liquid density, g·cm^3; g: gravitational acceleration, m·s^{-2}; h: gas inject depth, cm; P_V: vacuum chamber pressure, Pa	[37]

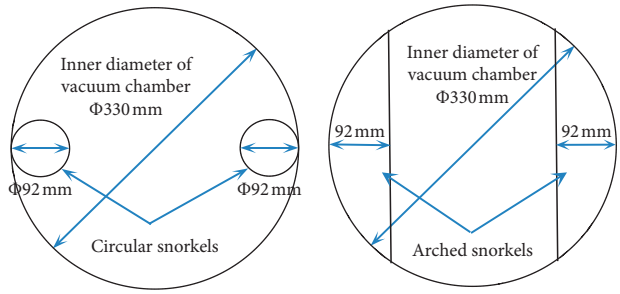

Figure 1: Model schematic of the RH vacuum chamber with (a) circular and (b) arched snorkels (top view).

Table 2: Parameters of the prototype and water model.

Item	Prototype (mm)	Water model for circular snorkels (mm)	Water model for arched snorkels (mm)
Diameter of ladle top	3077	564	564
Diameter of ladle bottom	2666	489	489
Height of ladle	3806	692	692
Inner diameter of vacuum chamber	1800	330	330
Height of vacuum chamber	10350	1000	1000
Internal diameter of circular snorkel	500	92	92
Internal diameter of arched snorkel	1800	330	330
Internal arc height of arched snorkel	500	92	92
Length of snorkels	1500	275	275
Inner diameter of gas injection nozzles	6	1.1	1.1
Distance between nozzles and bottom of vacuum chamber	550	100	100

(XC-LSB-1, XINGLIANCHEN Technology Co., Ltd., China). Each measurement was repeated three times, and the cross-sectional velocity was obtained by the average value of all measuring points. The circulation flow rate was the product of the measured velocity and cross-sectional area of the down-leg.

2.4.2. Mixing Time. The mixing time T_{mix} was measured by an electrical conductivity meter [18, 36]. The saturated NaCl aqueous solution was used as the tracer. When the fluid flow in the model was stable, the saturated NaCl aqueous solution was injected into the water through the spare nozzle on top of up-leg. Meanwhile, the conductivity instrument (DDS-307A, INESA Scientific Instrument Co., Ltd., China) was employed to measure the conductivity until a stable value (C_∞) was reached. The time for reaching the stable value is called mixing time. The conductivity probe was placed 60 mm below the ladle liquid level in the center between the up-leg and down-leg.

2.5. RH Work Principle and Bubble Behavior. The lifting gas is injected into the molten steel through the nozzles, and discrete spherical bubbles are formed at the nozzle exit. The bubbles with initial horizontal velocity enter into up-leg from the nozzles, and then the bubbles float upward and drive the molten steel up. Figure 3 shows the schematic of the bubble formation and motion path.

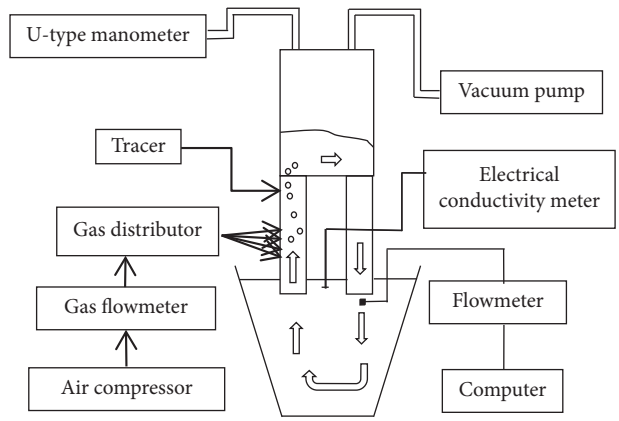

Figure 2: Schematic of water modeling.

Table 3: Parameters of the prototype and water model.

Main parameters	Vacuum degree (Pa)	Gas flow rate ($Nm^3 \cdot h^{-1}$)						Insertion depth of snorkel (mm)			
Prototype	67	35	69	104	138	173	193	382	545	710	818
Model	97709	0.5	1	1.5	2	2.5	2.8	70	100	130	150

The molten steel circulation process between the vacuum chamber and the ladle in RH vacuum degasser is similar to the "bubble pump" mechanism. A certain height difference between the liquid levels in the vacuum chamber and ladle is created in the vacuum degree of the vacuum chamber. The lifting gas first enters into molten steel in the form of bubbles, floats upward, and then expands with the temperature increase and pressure decrease. Accordingly, the density of gas-liquid two-phase in the up-leg reduces. The molten steel in the ladle is driven to the up-leg and then flows out through the down-leg due to gravity after entering the vacuum chamber. Thereafter, a circulation flow is formed, and the following equation is achieved [8, 14, 17]:

$$A_{\text{gas}} = A_{\text{steel}} + A_{\text{loss}}, \tag{2}$$

where A_{gas} is the gas expansion work, J; A_{steel} is the work for lifting molten steel, J; and A_{loss} is the lost work, J.

Considering A_{loss} is small, equation (2) can be expressed as

$$A_{\text{gas}} = A_{\text{steel}} = MHg = M\left(\frac{P_0 - P}{\rho_{g-1}}\frac{P_0 - P}{\rho_1}\right), \tag{3}$$

where M is the quality of lifting liquid steel, kg; H is the lifting height of liquid steel, m; P_0 is the atmospheric pressure, Pa; g is the acceleration of gravity, $m \cdot s^{-2}$; P is vacuum chamber pressure, Pa; $\rho_{g\text{-}1}$ is the density of gas-liquid two-phase, $kg \cdot m^{-3}$; and ρ_l is the density of liquid, $kg \cdot m^{-3}$. The density of the gas-liquid two-phase is the weighted value of the gas and liquid phases and obtained from equation (4) [17] as follows:

$$\rho_{g-1} = \alpha \cdot \rho_g + (1 - \alpha) \cdot \rho_1, \tag{4}$$

where α is the gas holdup.

3. Results and Discussion

3.1. Comparison of RH with Circular Snorkels and RH with Arched Snorkels

3.1.1. Flow Field. Under the condition of vacuum chamber pressure ($P = 97709$ Pa), insertion depth of snorkel ($H_{\text{imm}} = 100$ mm), gas flow rate ($Q_{\text{m}} = 1.0$ $Nm^3 \cdot h^{-1}$), and flow field using the black ink as tracer is shown in Figure 4. The ink was injected into up-leg through the spare nozzle on the top of up-leg. A high-speed camera was used to record the flow field. As shown in the flow fields from the water models, the molten steel driven by lifting gas flowed into the vacuum chamber through the up-leg, and violent mixing occurred in the vacuum chamber. Then, the molten steel flowed downward the ladle through down-leg, reached the ladle bottom, and rose upward again. The time of tracer in RH with arched snorkels to complete the mixing in the vacuum chamber, reaching the ladle bottom and complete one cycle, was, respectively, 3 s, 12 s, and 18 s and that of RH with circular snorkels was 3 s, 18 s, and 44 s. Compared with RH with circular snorkels, the quantity of the flowing molten steel through down-leg increases with the increase of the cross-sectional area and has a better diffusion capacity in the ladle while flowing to the bottom of the ladle in RH with arched snorkels. The mixing capacity of RH with arched snorkels was stronger than that of RH with circular snorkels.

3.1.2. Saturated Gas Flow Rate. In water model experiment, the circulation flow rate increases with the gas flow rate. After reaching a certain value, the circulation flow rate tends to be saturated. The circulation flow rate at this time is called saturated circulation flow rate $G_{m,\max}$, and the minimum gas flow rate corresponding to the $G_{m,\max}$ is called saturated gas flow rate $Q_{m,\max}$ [14, 36].

The horizontal section and horizontal trajectory of the bubbles in gas-liquid plume observed schematically at the

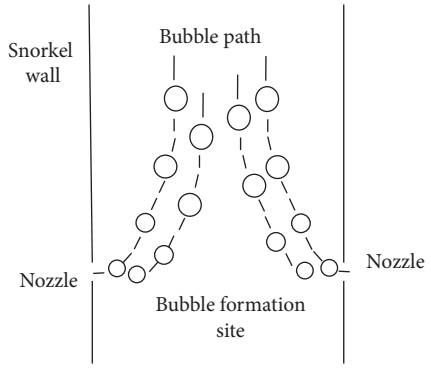

Figure 3: Schematic of the formation and path of bubbles in up-leg.

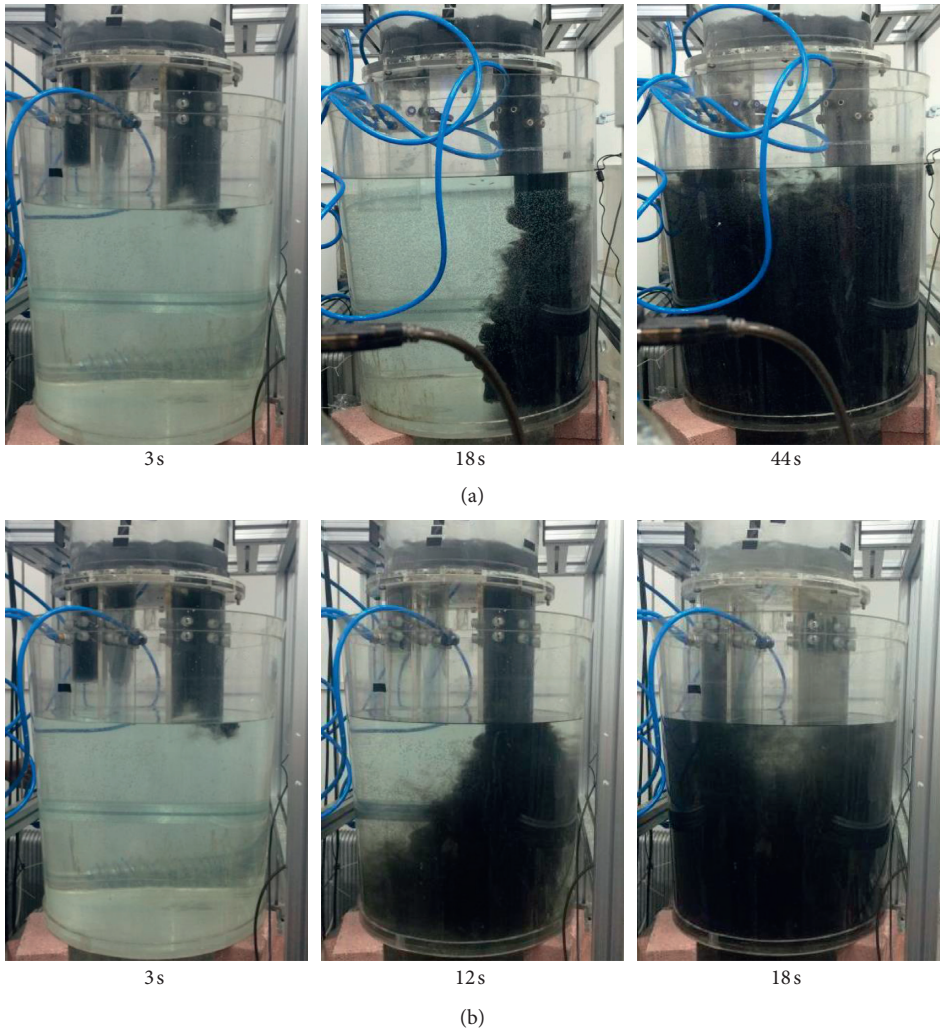

Figure 4: Flow field of (a) RH with circular snorkels and (a) RH with arched snorkels in one circulation.

outlet of the up-leg are shown schematically in Figure 5. For the two RH models, the bubbles in the gas-liquid plume formed at the exit of each nozzle are individually close to the wall of up-leg at small gas flow rate. With the increase of the gas flow rate, the diameter and horizontal penetrating depth of bubbles in gas-liquid plume increase. When the gas flow rate tends to be $Q_{m,\max}$, the bubbles in gas-liquid plume will collide with each other for RH with circular snorkels as shown in Figure 5(a), and bubbles from nozzle 2 and 3 will collide the opposite wall lastly for RH with arched snorkels as shown in Figure 5(b). If the gas flow rate continues to increase and the bubbles are in the state of ejection, the gas driving power will be greatly reduced and the circulation flow rate will tend to be saturated. Therefore, it can be

considered that the gas flow rate corresponding to the contact of bubbles from different nozzles with each other or the contact of bubbles and opposite wall is $Q_{m,\max}$. The bubble is simulated by a complete sphere, and the geometric conditions of this contact state of RH with circular snorkels and RH with arched snorkels are expressed by equations (5) and (6) [10]. Equations (7)–(9) [37] show the calculation formulas of diameter and horizontal penetrating depth of bubble; by combining equations (5) and (6), the $Q_{m,\max}$ of the two RH water models can be calculated:

$$d_B = \left(\frac{d_p}{2 - L_B} + \frac{d_B}{2}\right) * 2\sin\left(\frac{\theta_N}{2}\right), \tag{5}$$

$$\frac{d_p/2 - H_s}{\cos(\theta_N/2)} + L_B = \frac{d_p}{2}, \tag{6}$$

where d_B is the bubble diameter, m; d_p is the diameter of up-leg, m; L_B is the horizontal penetrating depth of bubble, m; H_s is internal arc height; and θ_N is the angle between adjacent nozzles; for circular snorkel,$\theta_N = 2\pi/n_c$ (n_c is the nozzle number); for arched snorkel, $\theta_N = \arccos[(0.5d_p - H_s)/0.5d_p]/2.5$:

$$d_B = \left[\left(\frac{6\sigma d_0}{\rho_1 g}\right)^2 + \left\{0.54\left[\frac{Q_g}{4n}d_0^{0.5}\right]^{0.289}\right\}^6\right]^{1/6}, \tag{7}$$

$$\frac{L_B}{d_0} = 3.7\left[\frac{\rho_g}{\rho_1 - \rho_g}\frac{V_g^2}{g d_0}\right]^{1/3}, \tag{8}$$

$$V_g = \frac{Q_g/n}{\pi d_0^2/4}, \tag{9}$$

where d_0 is the nozzle diameter, m; σ is the surface tension in the liquid phase, $N{\cdot}m^{-1}$; ρ_1 and $\rho_g$are the density of liquid and phase, $kg{\cdot}m^{-3}$; n is the nozzle number; V_g is the orifice gas velocity, $m{\cdot}s^{-1}$; $g$is the acceleration of gravity, $m{\cdot}s^{-2}$; and Q_g is the gas flow rate, $Nm^3{\cdot}s^{-1}$.

The $Q_{m,\max}$ of RH with circular snorkels calculated from above is 2.52 $Nm^3{\cdot}h^{-1}$. And, this is 5.03 $Nm^3{\cdot}h^{-1}$ to RH with arched snorkels. The $Q_{m,\max}$ of RH with arched snorkels is approximately 99.6% higher than that of the RH with circular snorkels from theoretical calculations.

Figure 6(a) shows the variation of circulation flow rate G_m and gas flow rate Q_m under the conditions that insertion depth of snorkel H_{imm} is 70, 100, 130, and 150 mm, respectively. The G_m increased with the increase of H_{imm}, and the G_m of RH with circular snorkels showed saturation tendency at about 2.50 $Nm^3{\cdot}h^{-1}$ of Q_m even at different H_{imm}, which was very consistent with the calculated value (2.52 $Nm^3{\cdot}h^{-1}$). The $Q_{m,\max}$ is the result of the horizontal movement of the bubbles and is independent of the insertion depth of snorkel. Therefore, Figure 6(b) only shows the variation of the G_m and Q_m under the condition of H_{imm} 70 mm; the G_m kept increasing with the increase of Q_m, because the $Q_{\text{m,max}}$ of RH with arched snorkels was 5.03 $Nm^3{\cdot}h^{-1}$.

According to equation (1), the $Q_{p,\max}$ of RH with arched snorkels is 347 $Nm^3{\cdot}h^{-1}$ on-site, which is far beyond the gas flow rate (60 ~ 130 $Nm^3{\cdot}h^{-1}$) in the production site. Excessive gas flow rate will result in mismatching of vacuum pump and other equipment. Therefore, it is not necessary to extend the gas flow rate to its $Q_{m,\max}$ of RH with arched snorkels in this physical simulation.

3.1.3. Circulation Flow Rate and Mixing Time. Under the condition of vacuum chamber pressure (P = 97709 Pa) and insertion depth of snorkel (H_{imm} = 100 mm), the relationship between the circulation flow rate G_m and gas flow rate Q_m in RH with arched snorkels and RH with circular snorkels is compared in Figure 7. It can be seen that the G_m of RH with arched snorkels was much larger than that of RH with circular snorkels in the whole Q_m. Under the same experimental conditions, the G_m of RH with arched snorkels was 2.0 ~ 2.8 times that of RH with circular snorkels. This result indicated that the G_m increases with the cross-sectional area increase of the arched snorkel; such result verified the previous studies that the circulation flow rate increases with the increase of cross-sectional area of the snorkel [3, 24, 38].

Under the condition of P = 97709 Pa and H_{imm} = 100 mm, the relationship between mixing time T_{mix} and Q_m in RH with arched snorkels and RH with circular snorkels is compared in Figure 8. It can be seen that the T_{mix} decreased with the increase in Q_m. When the Q_m was 2.0 $Nm^3{\cdot}h^{-1}$, the T_{mix} of RH with arched snorkels was 74 s, whereas that of RH with circular snorkels was 118 s. Under the experimental condition, the T_{mix} of RH with arched snorkels was 63% ~ 70% that of RH with circular snorkels.

3.2. Effect of Gas Flow Rate and Insertion Depth of Snorkel on RH with Arched Snorkels. The G_m increases with the increase of Q_m and H_{imm}. Equations (7)–(9) demonstrate that the bubble number, diameter, and horizontal penetrating depth increase with the increase in Q_m, the work conducted by bubble floatage increase. Accordingly, the "drove efficiency" to molten steel of the lifting gas and the G_m increase. When other parameters are fixed, the liquid level in vacuum chamber increases with the H_{imm}. The rising distance of the bubble increases and the contact time with the molten steel is longer, and the "drove efficiency" to molten steel of lifting gas increases, so the G_m increases.

However, H_{imm} should be controlled; otherwise, the gas lifting efficiency will be inefficient. The experimental results showed that the G_m rapidly increases with the H_{imm} increase when the Q_m was small. The H_{imm} influence on the G_m gradually decreased with the Q_m increase. Figure 9(a) shows when the H_{imm} exceeded 100 mm, especially when the Q_m was greater than 2.3 $Nm^3{\cdot}h^{-1}$, the H_{imm} increasing had little significance to G_m. With H_{imm} increase, the travel of bubbles increases, A_{loss} increases when the Q_m is fixed, and A_{steel} will decrease according to equation (2). The H_{imm} should be ≤100 mm and ≤550 mm on-site, which will improve the production efficiency of RH with arched snorkels.

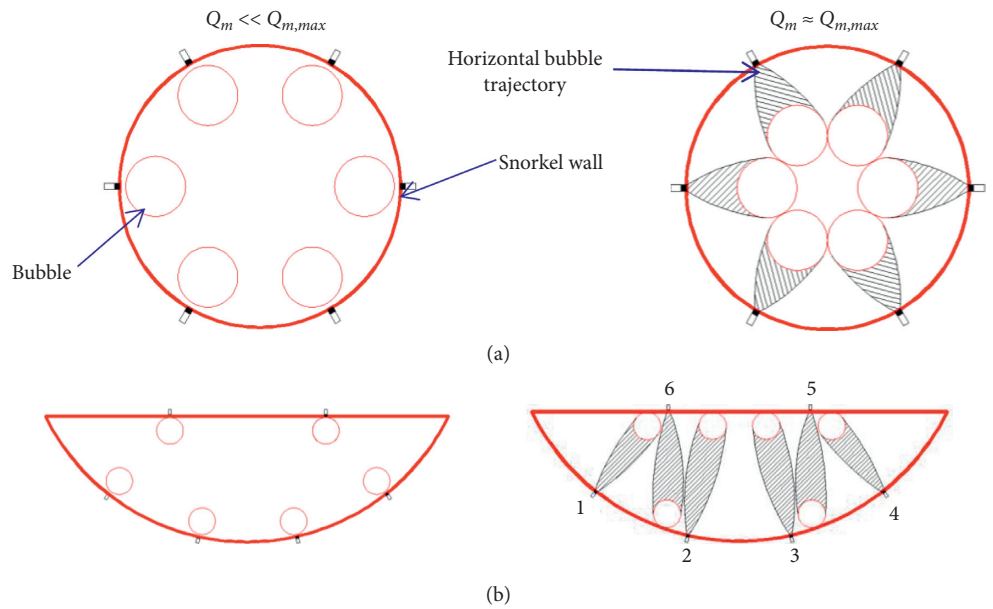

Figure 5: Illustration of bubble dispersion behavior in up-leg observed from the bath bottom. RH with (a) circular snorkels and (b) arched snorkels.

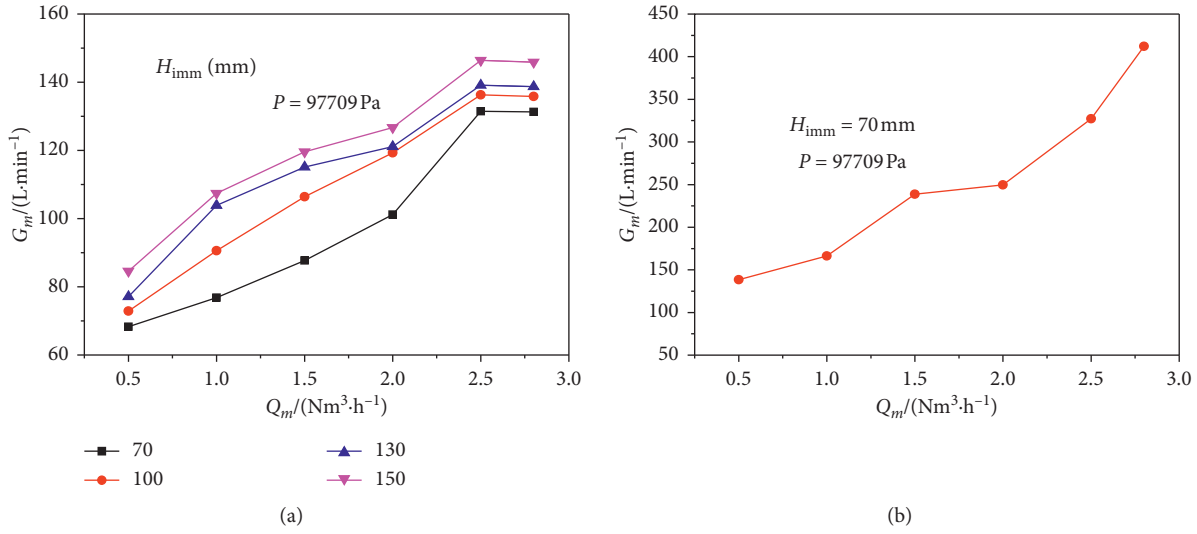

Figure 6: Variation of circulation flow rate G_m as a function of gas flow rate Q_m. (a) RH with circular snorkels. (b) RH with arched snorkels.

The T_{mix} decreased with the increase of the Q_m and H_{imm} as shown in Figure 9(b). The mixing time was obviously shortened with the increase of Q_m. The G_m increases with the increase of the Q_m, and the downflow of molten steel into the ladle from the vacuum chamber increases, which increases the stirring of molten steel and reduces the T_{mix}. The T_{mix} decreased with the H_{imm} increase at a certain vacuum degree as shown in Figure 9(b). When the H_{imm} was greater than 100 mm, the trend of T_{mix} decreasing was weakened. This finding indicates that the H_{imm} of the arched snorkels should be ≤ 550 mm on-site. The result of immersion depth control in the mixing time experiment is consistent with that in the circulation flow rate experiment.

Compared with then RH with circular snorkels, the RH with arched snorkels greatly improves the circulation flow rate, reduces the mixing time, and improves the mixing capacity. However, the refractory building is highly demanded. The RH with arched snorkels is seldom applied on-site because the complex structure of arched snorkels. The ability of the refractory building to resist molten steel erosion of RH with arched snorkels needs be studied in the future.

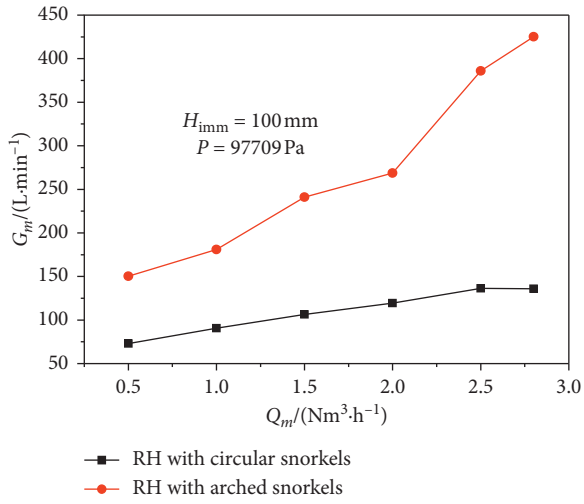

Figure 7: Relationship between G_m and Q_m in RH with arched snorkels and RH with circular snorkels.

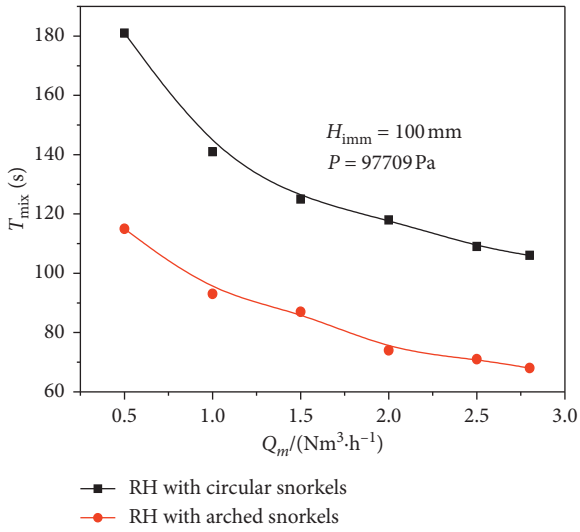

Figure 8: Relationship between Q_m and T_{mix} in RH with arched snorkels and RH with circular snorkel.

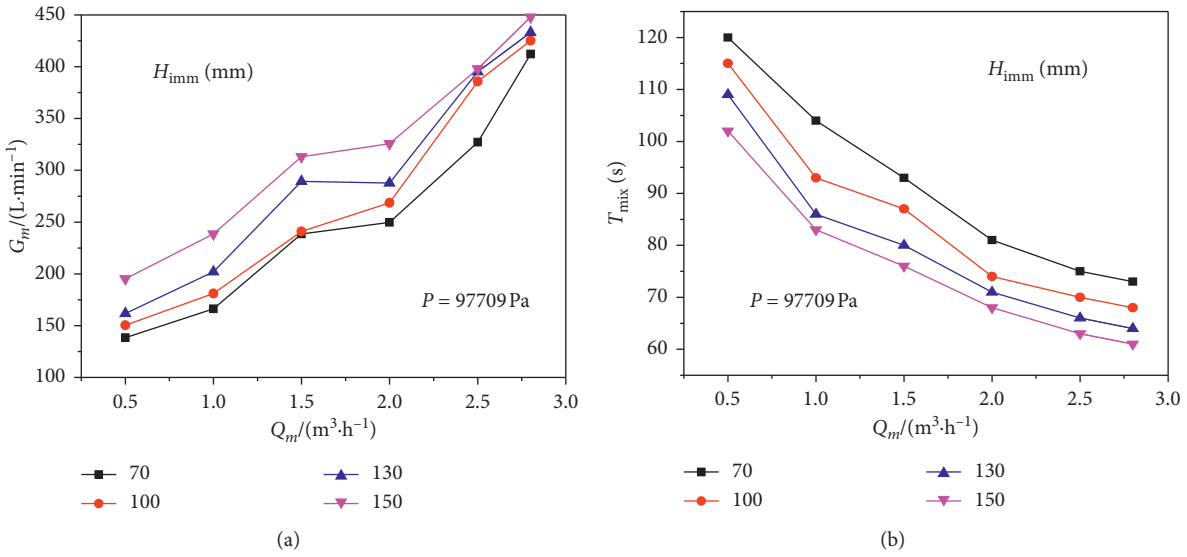

Figure 9: Effect of Q_m and H_{imm} on the G_m and T_{mix} of RH with arched snorkels.

4. Conclusions

(1) The circulation flow rate increases 100% ~ 180%, and the mixing time decreases by approximately 35% compared with RH with circular snorkels in the whole range of the gas flow rate.

(2) The saturated gas flow rate of RH with arched snorkels is 99.6% more than that of RH with circular snorkels, which can greatly increase the gas flow rate range on-site.

(3) Compared with the RH with circular snorkels, the quantity of the flowing molten steel through down-leg increases with the increase of the cross-sectional area and has better diffusion in the ladle while flowing to the bottom of the ladle. The RH with arched snorkels has stronger mixing capacity.

(4) The circulation flow rate increases, and the mixing time decreases with the increase of the gas flow rate and insertion depth. The insertion depth of the arched snorkel should be ≤ 550 mm on-site to improve the production efficiency.

Data Availability

The data used to support the findings of this study are available from the corresponding author upon request.

Conflicts of Interest

The authors declare no conflicts of interest.

Acknowledgments

The authors are grateful for support from the National Natural Science Foundation of China (Nos. U50704012, U1710257, and 51704203), Excellent Talents Science and Technology Innovation Project of Shanxi Province (No. 201605D211018), Scientific and Technological Innovation Programs of Higher Education Institutions in Shanxi (No. 2019L0656), Key Research and Development Project of Shanxi Province (No. 201903D121093), Science and Technology Innovation Project of Educational Commission of Shanxi Province (No. 2019L0616), and Doctoral Research Foundation of Taiyuan University of Science and Technology, China (No. 20142001).

References

[1] J. Pieprzyca, T. Merder, M. Saternus et al., "Physical Modelling Of The Steel Flow In RH Apparatus," *Archives of Metallurgy and Materials*, vol. 60, no. 3, pp. 1859–1863, 2015.

[2] M. Takahashi, H. Matsumoto, and T. Saito, "Mechanism of decarburization in RH degasser," *ISIJ International*, vol. 35, no. 12, pp. 1452–1458, 2007.

[3] Y. G. Park, K. W. Yi, and S. B. Ahn, "The effect of operating parameters and dimensions of the RH system on melt circulation using numerical calculations," *ISIJ International*, vol. 41, no. 5, pp. 403–409, 2001.

[4] Y. Luo, C. Liu, Y. Ren, and L. Zhang, "Modeling on the fluid flow and mixing phenomena in a RH steel degasser with oval down-leg snorkel," *Steel Research International*, vol. 89, no. 12, Article ID 1800048, 2018.

[5] D. Q. Geng, H. Lei, and J. C. He, "Numerical simulation of the multiphase flow in the rheinsahl-heraeus (RH) system," *Metallurgical and Materials Transactions B*, vol. 41, no. 1, pp. 234–247, 2010.

[6] L. C. Trindade, J. J. M. Peixoto, C. A. da Silva et al., "Influence of obstruction at gas-injection nozzles (number and position) in RH degasser process," *Metallurgical and Materials Transactions B*, vol. 50, no. 1, pp. 578–584, 2019.

[7] X. G. Ai, Y. P. Bao, W. Jiang, J. H. Liu, P. H. Li, and T. Q. Li, "Periodic flow characteristics during RH vacuum circulation refining," *International Journal of Minerals, Metallurgy, and Materials*, vol. 17, no. 1, pp. 17–21, 2010.

[8] S. K. Ajmani, S. K. Dash, S. Chandra et al., "Mixing evaluation in the RH process using mathematical modelling," *Transactions of the Iron & Steel Institute of Japan*, vol. 44, no. 1, pp. 82–89, 2007.

[9] Y. Kato, H. Nakato, T. Fujii, S. Ohmiya, and S. Takatori, "Fluid flow in ladle and its effect on decarburization rate in RH degasser," *ISIJ International*, vol. 33, no. 10, pp. 1088–1094, 1993.

[10] W. Zheng, Z. P. He, G. Q. Li et al., "Physical simulation of effect of injection parameters on circulation flow rate and mixing time in RH vacuum refining process," *Journal of Iron & Steel Research*, vol. 29, no. 5, pp. 373–381, 2017.

[11] G. Tokio, H. Katoh, M. Tetsuo et al., "Mixing of molten steel in a ladle with RH reactor by the water model experiment," *Denki Seiko*, vol. 50, no. 2, pp. 128–137, 1979.

[12] H. Ono-Nakazato, H. Tajiri, T. Usui et al., "Rate enhancement of the degassing reaction by the enlargement of RH and DH reactors," *Tetsu-to-Hagane*, vol. 89, no. 11, pp. 1113–1119, 2009.

[13] R. Tsujino, M. J. Nakashima, and I. Sawada, "Numerical analysis of molten steel flow in ladle of RH process," *ISIJ International*, vol. 29, no. 7, pp. 589–595, 1989.

[14] J. H. Wei, N. W. Yu, and Y. Y. Fan, "Study on flow and mixing characteristics of molten steel in RH and RH-KTB refining processes," *Journal of Shanghai University (English Edition)*, vol. 6, no. 2, pp. 167–175, 2002.

[15] T. Kuwabara, K. Umezawa, K. Mori, and H. Watanabe, "Investigation of decarburization behavior in RH-reactor and its operation improvement," *Transactions of the Iron and Steel Institute of Japan*, vol. 28, no. 4, pp. 305–314, 1988.

[16] B. Li and F. Tsukihashi, "Modeling of circulating flow in RH degassing vessel water model designed for two- and multi-legs operations," *ISIJ International*, vol. 40, no. 12, pp. 1203–1209, 2000.

[17] V. Seshadri, C. A. Silva, and I. A. Da Silva, "Physical modeling simulations of refining processes in Brazilian Steel Industry," *Scandinavian Journal of Metallurgy*, vol. 34, no. 6, pp. 340–352, 2005.

[18] L. Lin, F. Bao, L. Q. Zhang, and H. L. Ou, "Physical model of fluid flow characteristics in RH-TOP vacuum refining process," *International Journal of Minerals, Metallurgy, and Materials*, vol. 19, no. 6, pp. 483–489, 2012.

[19] H. Ling, C. Guo, A. N. Conejo et al., "Effect of snorkel shape and number of nozzles on mixing phenomena in the RH process by physical modeling," *Metallurgical Research & Technology*, vol. 114, no. 111, pp. 1–13, 2017.

[20] V. Seshadri, C. A. da Silva, I. A. da Silva, G. A. Vargas, and P. S. B. Lascosqui, "Decarburisation rates in RH-KTB degasser of CST steel plant through physical modelling study," *Ironmaking & Steelmaking*, vol. 33, no. 1, pp. 34–38, 2013.

[21] B. Zhu, D. Q. Liu, M. S XuRen, and B. Hu, "Effect of nozzle blockage on circulation flow rate in up-snorkel during the RH degasser process," *Steel Research International*, vol. 87, no. 2, pp. 136–145, 2015.

[22] K. Yang and J. Szekely, "A mathematical model of fluid flow and inclusion coalescence in the RH vacuum degassing system," *Transactions of the Iron & Steel Institute of Japan*, vol. 23, no. 6, pp. 465–474, 2006.

[23] H. Ling, L. Zhang, and C. Liu, "Mathematical modeling on the fluid flow during RH degassing process," *Metallurgical Research & Technology*, vol. 114, no. 4, pp. 510–519, 2017.

[24] J. H. Wei and H. T. Hu, "Mathematical modelling of molten steel flow in a whole degasser during RH refining process," *Ironmaking & Steelmaking*, vol. 32, no. 5, pp. 427–434, 2005.

[25] B. Li and H. Huo, "Homogenous flow model for gas driven circulating flow in RH refining system," *Acta Metallurgica Sinica*, vol. 41, no. 1, pp. 60–66, 2005.

[26] H. Ling, L. Zhang, and C. Liu, "Effect of snorkel shape on the fluid flow during RH degassing process: mathematical modelling," *Ironmaking & Steelmaking*, vol. 45, no. 4, pp. 1–12, 2016.

[27] H. Ling, F. Li, L. Zhang, and A. N. Conejo, "Investigation on the effect of nozzle number on the recirculation rate and mixing time in the RH process using VOF + DPM model," *Metallurgical and Materials Transactions B*, vol. 47, no. 3, pp. 1950–1961, 2016.

[28] M. K. Mondal, N. Maruoka, S. Kitamura, G. S. Gupta, H. Nogami, and H. Shibata, "Study of fluid flow and mixing behaviour of a vacuum degasser," *Transactions of the Indian Institute of Metals*, vol. 65, no. 3, pp. 321–331, 2012.

[29] L. Zhang and F. Li, "Investigation on the fluid flow and mixing phenomena in a ruhrstahl-heraeus (RH) steel degasser using physical modeling," *JOM*, vol. 66, no. 7, pp. 1227–1240, 2014.

[30] X. G. Ai, S. L. Li, N. Wang, and N. Lv, "Simulation of inclusions removal influenced by snorkel and blowing parameters in RH refining," *Advanced Materials Research*, vol. 291, no. 294, pp. 155–158, 2011.

[31] Z. You, G. Cheng, X. Wang, Z. Qin, J. Tian, and J. Zhang, "Mathematical model for decarburization of ultra-low carbon steel in single snorkel refining furnace," *Metallurgical and Materials Transactions B*, vol. 46, no. 1, pp. 459–472, 2015.

[32] G. Chen, S. He, Y. Li, and Q. Wang, "Modeling dynamics of agglomeration, transport, and removal of Al_2O_3 clusters in the rheinsahl-heraeus reactor based on the coupled computational fluid dynamics-population balance method model," *Industrial & Engineering Chemistry Research*, vol. 55, no. 25, pp. 7030–7042, 2016.

[33] J. H. Wei and N. W. Yu, "Mathematical modelling of decarburisation and degassing during vacuum circulation refining process of molten steel: application of the model and results," *Steel Research*, vol. 73, no. 4, pp. 143–148, 2002.

[34] P. H. Li, Q. J. Wu, W. H. Hu et al., "Mathematical simulation of behavior of carbon and oxygen in RH decarburization," *Journal of Iron and Steel Research International*, vol. 22, no. S1, pp. 63–67, 2015.

[35] H. Watanabe, K. Asano, and T. Saeki, "Some chemical engineering aspects of R-H degassing process," *Tetsu-to-Hagane*, vol. 54, no. 13, pp. 1327–1342, 1968.

[36] V. Seshadri and S. L. Costa, "Cold model studies of R.H. degassing process," *Transactions of the Iron and Steel Institute of Japan*, vol. 26, no. 2, pp. 133–138, 1986.

[37] C. Kamata, S. Hayashi, and K. Ito, "Estimation of circulation flow rate in RH reactor using water model," *Tetsu-to-Hagane*, vol. 84, no. 7, pp. 484–489, 1998.

[38] S. Fan and B. Li, "Modeling of circulating flow in RH degassing vessel water model designed for two-and multi-leg operations," *Acta Metallrugica Sinica*, vol. 37, no. 10, pp. 1100–1106, 2001.

[39] D. Q. Geng, J. X. Zheng, K. Wang et al., "Simulation on decarburization and inclusion removal process in the ruhrstahl-heraeus (RH) process with ladle bottom blowing," *Metallurgical and Materials Transactions B*, vol. 46, no. 3, pp. 1484–1493, 2015.

[40] D. Q. Geng, X. Zhang, X. A. Liu et al., "Simulation on flow field and mixing phenomenon in single snorkel vacuum degasser," *Steel Research International*, vol. 86, no. 7, pp. 724–731, 2015.

[41] P. A. Kishan and S. K. Dash, "Prediction of circulation flow rate in the RH degasser using discrete phase particle modeling," *ISIJ International*, vol. 49, no. 4, pp. 495–504, 2009.

[42] G. Dian-Qiao, L. Hong, and H. Ji-Cheng, "Application of MHD phenomenon on secondary refining and continuous casting process," *Journal of Iron and Steel Research(International)*, vol. 49, no. S2, pp. 941–944, 2012.